Med Chem Res
DOI 10.1007/s00044-015-1328-6

MEDICINAL CHEMISTRY RESEARCH

ORIGINAL RESEARCH

High-throughput virtual screening, identification and in vitro biological evaluation of novel inhibitors of signal transducer and activator of transcription 3

Pushpendra Singh · Felix Bast

Received: 20 October 2014 / Accepted: 17 January 2015

Abstract Signal transducer and activator of transcription (STAT) family, encompassing protein molecules that function as a second messenger and transcription factor, are famously known to regulate a multitude of cellular processes including inflammation, cell proliferation, invasion, angiogenesis, metastasis and immune system homeostasis. STAT3 is one of the six members of a family of transcription factors. STAT3 has proved themselves to be interesting candidates for anticancer therapy as they are over-expressed in most cancer cells. Thus, we studied receptor-based molecular docking of STAT3 against natural compounds and further validations of lead molecules in an array of cancer cells. In the present study, we screened approximately 50,000 natural compounds from the IBS. All natural compounds were docked with the X-ray crystal structure of STAT3 (PDB; 1BG1) retrieved from the protein data bank by using Maestro 9.6 (Schrödinger Inc). First, we performed high-throughput virtual screening of IBS against the SH2 domain of STAT3. Further, best 20 compounds that possess minimal Gscore along with 85 natural compounds that had been reported in published literature as having anticancer properties were selected, and molecular docking was performed using the XP (extra precision) mode of GLIDE. We analyzed Gscore and protein–ligand interactions of top ranking compounds. It was discovered in this study, compounds CID252682, CID5281670 (Morin), CID5281672 (Myricetin), CID72277 (Epigallocatechol) and CID65064 (Epigallocatechin Gallate, EGCG) yielded the excellent dock score with the STAT3 concluded with the help of docking-free energy. Moreover, IBS STOCK1N-43090, STOCK1N-66505, STOCK1N-54303, STOCK1N-44634, STOCK1N-45027, STOCK1N-73784, STOCK1N-69597, STOCK1N-73062, STOCK1N-81915 and STOCK1N-70844 have better docking-free energy. Further, we chose EGCG and myricetin compounds, and their effect on biological activity such as cell proliferation, oxidative stress, colony formation, mRNA expression of STAT3, and cell number was reported after the 48 h treatments in cancer cell lines. EGCG and myricetin reduce the STAT3 mRNA expression confirmed by RTPCR. Moreover, EGCG and myricetin reduce cell proliferation and ROS generation after 48 h treatments. Interestingly, our result also indicates that the reduction in potential for colony formation enhances anti-metastasis activity of EGCG and myricetin. The information obtained from our study assisted us in drawing a more lucid picture regarding the existence STAT3 natural compounds inhibitor on diverse cancer cells.

Keywords
Signal transducer and activator of transcription · Natural compounds · Inter Bio Screen natural compound library (IBS) · Maestro 9.6

Introduction

STAT pathway in its role as a second messenger is a well-known cell signaling cascade involved in regulating numerously cellular processes, viz. growth, development, and maintenance of immune system homeostasis, in

Electronic supplementary material The online version of this article (doi:10.1007/s00044-015-1328-6) contains supplementary material, which is available to authorized users.

P. Singh · F. Bast (✉)
Centre for Biosciences, School of Basic and Applied Science, Central University of Punjab, Bathinda 151001, Punjab, India
e-mail: felix.bast@gmail.com; felix.bast@cup.ac.in

Published online: 31 January 2015

addition to numerous intracellular signaling pathways, including that of cytokine and growth factor (Simon *et al*., 1998). STAT family comprises of proteins characterized by their ability to act as (1) signal transducers (second messengers) and (2) transcription factors, without which cell proliferation, differentiation and cell migration would not occur. Eight mammalian STAT proteins are commonly known that mediate the expression of important proto-oncogenes by virtue of their function to act as transcription factors (TF), which are in-turn activated by a variety of cytokines, hormones and growth factors. STAT pathway finds its utility in maintaining the hematopoiesis of the body, immune system homeostasis, sexually dimorphic growth regulation, along with other physiological processes that participate actively in the initiation and progression of complex diseases including diabetes and cancer (Rawlings *et al*., 2004). There are two types of ligand–receptor interactions in STAT pathway which are classified on the basis of downstream activation of signaling molecules. In ligands such as erythropoietin and growth hormone, the receptor subunits are bound as homodimers, whereas for other ligands such as interferons and interleukins, the receptor subunits are heteromultimeric (Huang *et al*., 2005a; Watowich *et al*., 1994). Uncontrolled cell growth, development and immune responses of the body may occur as a consequence of deregulation of STAT family accredited to over-expression or functional impairment of the molecules. Members of the STAT family range in size from 750 to 900 amino acids and contains several structural domains including SH2 domain (Takeda and Akira, 2000), coiled-coil, DNA-binding, linker, tyrosine activation and transcriptional activation domains (Becker *et al*., 1998). STAT3, STAT4, STAT5 and STAT6 play a critical role in the complex diseases like cancer and diabetes and are believed to possess pro-proliferative and anti-inflammatory associated activities which are thought to be crucial for successful regulation of proliferation and differentiation of the cells (Friedbichler *et al*., 2009; Gooch *et al*., 2002; Grivennikov and Karin, 2010; Schindler *et al*., 2007; Takeda *et al*., 1997). However, aberrant signaling by STAT3 has been reported in a variety of malignancies, including the breast and prostate cancer (Aggarwal *et al*., 2009; Azare *et al*., 2007; Huang *et al*., 2005b; Yue and Turkson, 2009). Consequently, it is reported that over-activated STAT3 and STAT5 increase tumor cell proliferation and invasion while suppressing anti-tumor immunity (Yu *et al*., 2007, 2009).

Several lines of evidence such as genetically engineered mutant of STAT3 and dominant-negative variant of STAT3 experimental approaches that block the over-activation of STAT3 led to obstruction of tumor growth confirmed the STAT3 as a target for cancer drug discovery (Niu *et al*., 1999, 2001; Zhang *et al*., 2013). It is suggested that inhibition of STAT3 by a selective small molecule decreased the tumor volume and prolongation of the time to tumor recurrence (Dave *et al*., 2012; Ni *et al*., 2000). By using several approaches, nucleotide and non-nucleotide-based STAT inhibitors are being developed and undergoing clinical evaluation for the treatment of various cancers. However, due to a multitude of side effects and arguable efficacies, there is a demand for newer compounds for the treatment of cancer. A number of compounds have been suppressed the over-activation of STAT3 including Niclosamide, Nifuroxazide, Kahweol, WP1066 and Cryptotanshinone. These compounds inhibit STAT3 activation by various mechanisms such as STAT3 tyrosine phosphorylation, STAT3 recruitment to the receptor and dimerization, STAT3 nuclear translocation and STAT3–DNA binding and transcriptional activation (Chung *et al*., 1997; Debnath *et al*., 2012; Fletcher *et al*., 2008). We have focused our efforts to discover natural compounds that have the capability to disrupting translocation, dimerization of STAT3 and STAT3–DNA binding with potentially improving potency and specificity. In this context, our aim of the present work had been to find a natural compound that can be developed as a suitable STAT3 signaling pathway inhibitor by using molecular docking and in vitro studies.

Methodology

In silico procedures

Selection and preparation of ligands

In silico, molecular docking procedure adapted from our previous published article (Singh and Bast, 2014a, b). Selected candidate ligand molecules were divided into two groups: (a) natural compounds that had been reported in the published literature (Bhanot *et al*., 2011; Cho and Park, 2008; Cragg and Newman, 2005; da Rocha *et al*., 2001; Hillman, 2012; Huang *et al*., 2012; Phosrithong and Ungwitayatorn, 2010; Roell and Baniahmad, 2011; Sarkar and Li, 2006; Sunil, 2012) and (b) IBS. IBS is a collection of one of the world's largest natural compound library, and in March 2013, it has grown to include over 50,000 compounds. Of the whole natural compound library, 60–65 % are compounds of plant origin; 5–10 % was isolated from microorganisms, about 5 % of marine species. These ligand molecules were subjected into ligand preparation by Ligprep wizard application of the Maestro 9.6 that performs amendment on the ligands, such as the addition of hydrogens, removal of water molecules, correction of bond lengths and bond angles. Pharmacokinetic properties of selected natural compounds are detailed in supplementary table 1.

Preparation of protein molecules

The X-ray crystal structure of STAT3(PDB; 1BG1) retrieved from the protein data bank (Becker *et al*., 1998). Maestro 9.6 protein preparation wizard applications accomplished for the correction of unprepared PDB structure, where changes such as addition of hydrogen atoms, assigning bond orders, creation of zero order bonds to metal, creation of disulphide bonds, fixing of the charges and orientation of groups were incorporated.

Molecular docking

Molecular docking studies using the selected ligand molecules were conducted using Maestro 9.6 molecular docking suite (Friesner *et al*., 2004, 2006; Halgren *et al*., 2004). Each of these selected compounds was docked into SH2 domain of STAT3 target protein molecules, and the docking conformation possessing the lowest energy was selected. After preparing protein and ligands, molecules energy minimization and optimization was done by using optimized potential for liquid simulations (OPLS_2005) force field (Jorgensen *et al*., 1996; Jorgensen and Tirado-Rives, 1988; Shivakumar *et al*., 2010) and one conformation for each ligand was generated as default setting of Maestro 9.6. After the completion of protein preparation, a receptor-grid file was generated. For running the grid generation module, we scaled van der waal radii of receptor atoms by 1.00 Å with a partial atomic charge of 0.25 as a default setting of Maestro 9.6. The active site of the receptor provides an accurate scoring function with thermodynamic optimal energy value and is calculated on a grid by various sets of fields. After the formation of receptor-grid file, molecular docking was performed. The final energy evaluation was done on the basis of Gscore.

ADME/T properties studies

ADME/T (Absorption, Distribution, Metabolism, Excretion, and Toxicity) properties were measured for the final screening of these lead compounds by using QikProp application of Schrödinger. Most of the drugs do not triumph in the late phase of clinical trials due to mediocre ADME properties such as poor compound solubility, gastric emptying time and intestinal absorption time. Thus, ADME properties of best-docked compounds were predicted using QikProp application of Schrodinger. QikProp application predicts properties such as log BB, overall CNS activity, Caco-2 and MDCK cell permeability and logKhsa for human serum albumin binding which are prerequisite for drug-like pharmacokinetic profile (Jorgensen and Duffy, 2002; Lu *et al*., 2004).

In vitro procedures

Chemicals

DMEM media, 1 % penicillin/streptomycin and fetal bovine serum (FBS) were purchased from Invitrogen. Ham's F-12 media were purchased from Himedia. EGCG purchased from MP Biomedicals Pvt Ltd and dissolved in dimethylsulfoxide (DMSO) as a 20-MM stock solution and diluted in culture medium to a final DMSO concentration of 0.25 % (vol/vol). Myricetin purchased from Sigma, Aldrich and dissolved in DMSO. TRIzol reagent purchased from life technologies, Gaithersburg.

Cell culturing

Hepatocellular carcinoma (HepG2), Lung carcinoma (A549 and H460) and Prostate cancer (PC3) human cell lines were obtained from NCCS, Pune (India). They were cultured in recommended medium supplemented with 10 % FBS, 1 % penicillin–streptomycin solution in a humidified 5 % CO_2 atmosphere at 37 °C. When adherent cells reached 80 % confluency, the cells were trypsinized using trypsin (0.25 %) and resuspended in medium supplemented with 10 % FBS, 1 % penicillin–streptomycin.

Total RNA isolation, cDNA synthesis, and quantitative RT-PCR

One million cells/well were plated into the six-well culture plate media containing 10 % FBS and 1 % penicillin–streptomycin and incubated at 37 °C overnight. After 24 h, incubation media were removed, and FBS-free media were added (serum starvation). After 24 h, media were replaced, and 80 μM of EGCG and myricetin treatment was done. Total RNA was extracted from cells using TRIzol. RNA pellet was dissolved in diethyl pyro-carbonate treated water and quantified at 260 nm/280 nm with thermo scientific nanodrop 2000 spectrophotometer. Yield and purity were verified by absorbance (optical density); absorption ratio A260 nm/A280 nm between 1.93 and 2.06 was considered for cDNA synthesis. For cDNA synthesis, one μg of total RNA was reverse-transcribed into cDNA using a high-capacity PrimeScript 1st strand cDNA Synthesis Kit (Takara Bio Inc). Gene expression was quantified by reverse transcription polymerase chain reaction (RT-PCR) using Applied Biosystems® Thermal Cyclers. Products of RT-PCR were separated by agarose gel electrophoresis to confirm correct amplification and size. Primer interactions with a templet cDNA were recognizing by using water and glyceraldehyde-3-phosphate dehydrogenase (GAPDH), and actin is used as a housekeeping gene to assure equal loading of the sample. The cycling parameters were

optimized as follows: PCR start at 60 °C for 2 min, followed by activation at 95 °C for 10 min, denaturing at 95 °C for 15 s, annealing at 60 °C for 45 s, elongation at 72 °C for 45 s, repeated for 38 amplification cycles and lastly final elongation at 72 °C for 5 min. PCR amplification products were separated with 2 % agarose gels.

Protocol for MTT assay

MTT assay detects the cell cytotoxicity via reduction in MTT by mitochondrial dehydrogenase to form thiazolyl blue formazan. 7×10^3 cells/well were seeded into the 96-well plate media containing 10 % fetal bovine serum and 1 % penicillin–streptomycin and then incubated at 37 °C overnight. After 24 h, incubation media were removed, and FBS-free media were added (serum starvation). The next day, media were replaced with 200 µL of fresh complete medium containing 5, 10, 20, 40 and 80 µM concentrations of EGCG and myricetin alone. After 48 h, the supernatants were removed, and cell were washed with PBS and incubated with MTT (100 µL, 0.5 mg/mL) in PBS for 4 h in a humidified atmosphere at 37 °C. 200 µL of dimethyl sulfoxide was added to dissolve the formazan crystals. The optical density (OD) of the colored solution was quantified at 570 nm wavelengths by using enzyme-linked immunoabsorbent assay reader (ELISA Synergy/H1).

Trypan blue exclusion assay

Trypan blue exclusion analysis was performed by using neubaurs chamber according to recommended protocol.

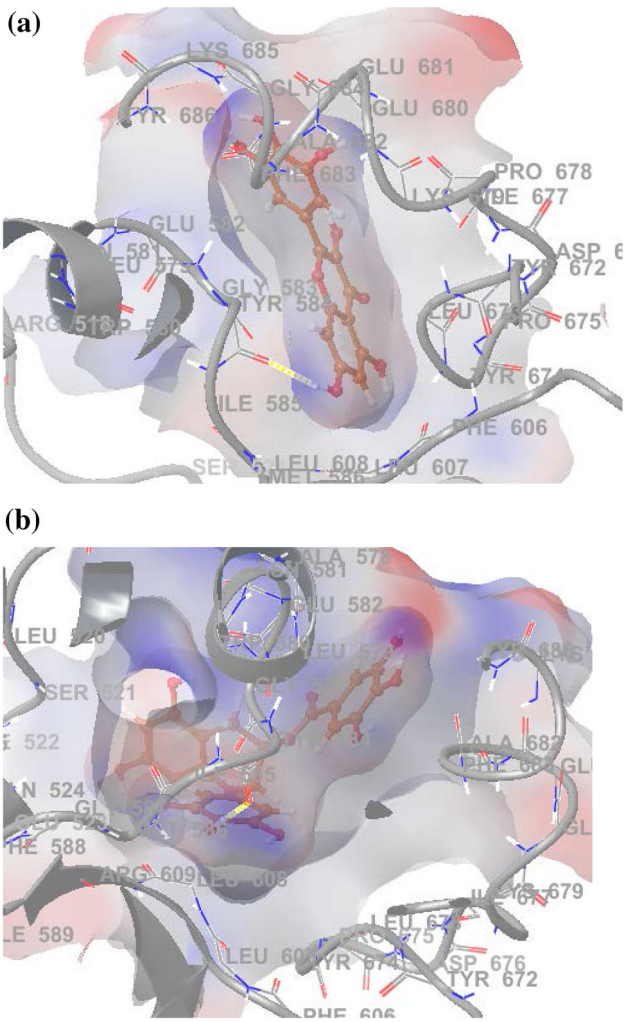

Fig. 1 Ribbon presentation of STAT3 (PDB; 1bg1) protein molecule with 5281672 (**a**) and 65064 (**b**)

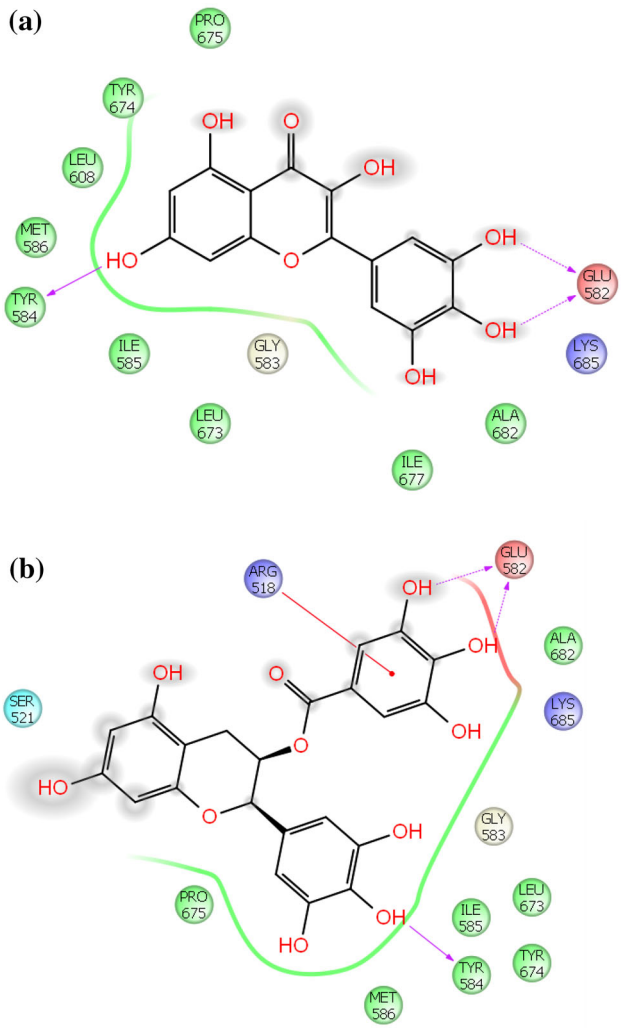

Fig. 2 Protein–ligands interactions profile of STAT3 (PDB; 1bg1) with CID5281672 and CID65064. Protein–ligands interactions profile revealed that myricetin and EGCG with SH2 domain of STAT3 amino acid Tyr585, Met586, Leu673, TYR674, Pro675, Ile677 and Ala682 involve the hydrophobic interactions. Furthermore, amino acid Ser521 and Glu582 included in side chain hydrogen bond and amino acid Gly583 and Tyr584 involved in back-bone hydrogen bone. Moreover, amino acid 518 and Tyr584 form pi-cation and pi–pi-cation interactions, respectively

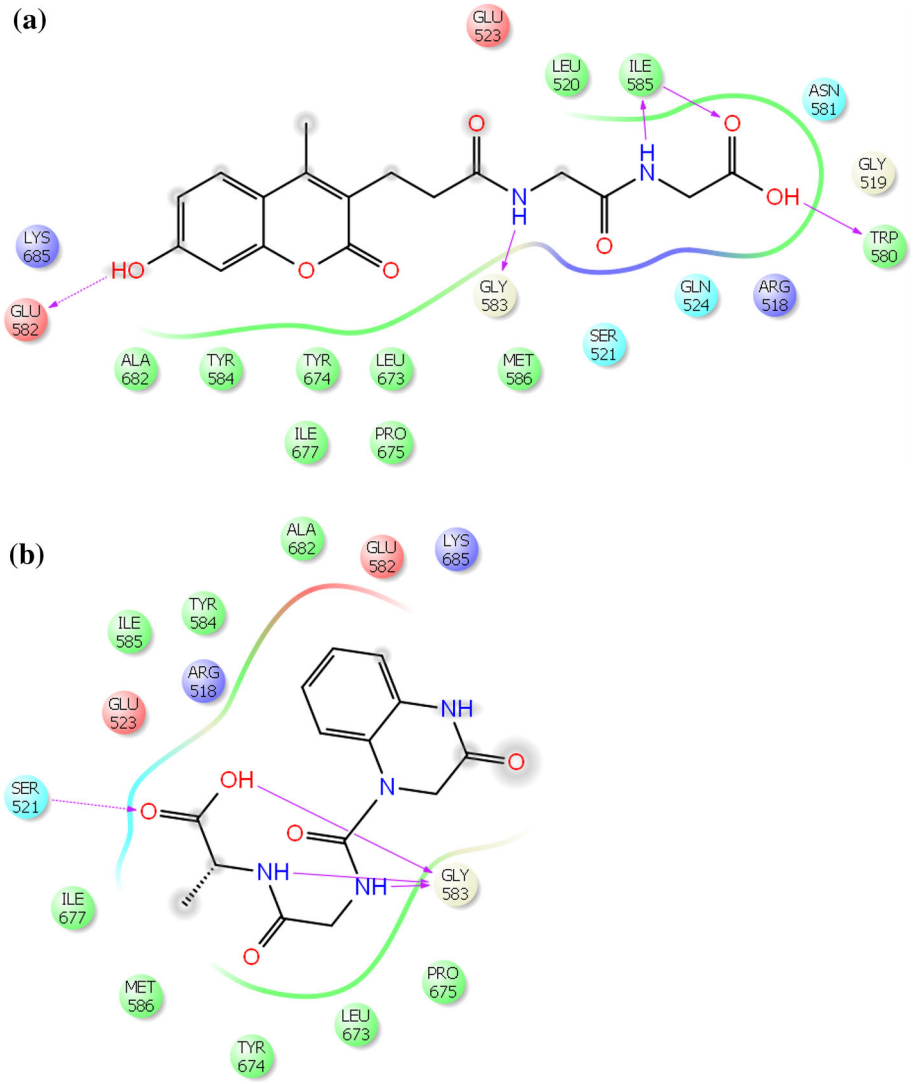

Fig. 3 Protein–ligand interactions profile of STAT3 (PDB; 1bg1) with STOCK1N-43090 and STOCK1N-66505

Cancer cells were plated at a cell density of approximately 2.5 × 104 cells/well in 6-well plates and grown with medium containing 10 % FBS. Twenty-four hrs after plating, the media was changed to media containing 0.5 % FBS in order to reveal the full effect of the compounds used. After serum starvation, cells were treated with compounds for 48 hrs. Control cancer cell cultures were treated with phosphate-buffered saline (PBS). 10 µL of cells sample and 10 µL of trypan blue stain mix very well and loaded 10 µL of the sample mixture into the half moon shaped neubaurs chamber and analyzed the live and dead cells.

Nitro blue tetrazolium (NBT) reduction assay

7×10^3 Cells/well were seeded into the 96-well tissue culture plates, media containing 10 % FBS and 1 % penicillin/streptomycin and then incubated at 37 °C overnight. After 24 h, incubation media were removed, and FBS-free media were added (serum starvation). After 24 h, the media were replaced with 200 µL of fresh complete medium containing 5, 10, 20, 40 and 80 µM concentrations of EGCG and myricetin. After 48 h, the supernatants were removed, and incubated with 100 µL 0.1 % NBT, and the plates were placed into an incubator for 4 h. The reduced NBT was solubilized with 100 µL 2 M KOH and 100 µL DMSO for 30 min. The absorbance was measured for each well at 570 nM using an ELISA Synergy/H1 plate reader.

Clonogenic assay

A Clonogenic assay was performed as described previously (Alimova *et al.*, 2009; Bill *et al.*, 2012; Liu *et al.*, 2007). Cells were seeded into six-well plates in triplicates at a

Table 1 Lowest binding energy for the ligand–SH2 domain of STAT3 (PDB; 1BG1) protein interactions as detected by GLIDE molecular docking

	Molecules	GScore	LipophilEvdW	HBond	Electro	Protein–ligand interactions
	CID5337997	−4.11	−2.46	−1.04	−0.36	Gly583 and Glu681
	CID252682	−4.01	−2.41	−1.52	−0.67	Glu582 and Tyr584
Control	CID11210478	−3.42	−2.54	−1.19	−0.25	Arg518 and Gly583
	CID114778	−3.11	−2.16	−0.48	−0.51	Glu582
	CID160254	−2.52	−2.62	0	0.01	
Anticancer agents	CID252682	−5.45	−2.95	−1.63	−0.88	Ser521 and Gly583
	CID5281670	−5.03	−2.74	−1.48	−0.71	Glu582 and Tyr584
	CID5281672	−4.83	−2.29	−1.59	−0.82	Glu582 and Tyr584
	CID72277	−4.82	−2.18	−2.07	−0.8	Glu582 and Tyr584
	CID65064	−4.78	−1.82	−2.88	−1.17	Arg518, Glu582 and Tyr584
	STOCK1N-43090	−6.46	−2.73	−2.37	−1.45	Trp580, Glu582, Gly583, and Ile585
IBS	STOCK1N-66505	−6.35	−2.48	−2.64	−1.07	Ser521 and Gly583
	STOCK1N-54303	−6.29	−3.08	−2.27	−1.16	Trp580, Gly583 and Ile585
	STOCK1N-44634	−6.1	−3.27	−2.19	−0.8	Trp580, Glu582, and Ile585
	STOCK1N-45027	−6.05	−3.15	−2.2	−0.97	Trp580, Gly583, and Ile585
	STOCK1N-73784	−5.87	−3.36	−1.69	−0.74	Trp580, Gly583, and Ile585
	STOCK1N-69597	−5.63	−3.26	−2.07	−0.64	Ser521, Gly583, and Tyr584
	STOCK1N-73062	−5.44	−2.83	−1.47	−0.81	Arg 518, Ser521, and Trp580
	STOCK1N-81915	−5.18	−2.1	−1.51	−0.91	Arg 518, Trp580, and Ile585
	STOCK1N-70844	−5.1	−3.16	−1.6	−0.87	Ser521 Trp580, Gly583, and Ile585

Molecule CID, Pubchem IDs; Molecule STOCK, InterBioScreen's library (IBS); GScore, Glide extra precision scores (kcal/mol); Lipophilic E Vdw, Chemscore lipophilic pair term and fraction of the total protein–ligand vdw energy; HBond, Hydrogen-bonding term; Electro, electrostatic rewards; Protein–ligands interactions, π–π stacking, π–cat interactions and hydrogen bond between the ligands and protein

density of 1×10^3cells/well in 2 ml of medium containing 10 % FBS. After 24 h, cultures were replaced with fresh medium containing 0.5 % FBS (control) and treatment (EGCG and myricetin) was done then incubated in a 37 °C humidified atmosphere containing 95 % air and 5 % CO_2, and grown for 3 weeks. Every second-day media were changed. The cell clones were stained for 15 min with a solution containing 0.5 % Giemsa stain and 25 % methanol, followed by rinse with water to remove excess dye. The colony numbers were counted by using an inverted microscope.

Data analysis and statistics

Statistical analysis was performed using SigmaPlot. The results of the in vitro experiments are expressed as mean ± SEM. Statistical analysis was done with ANOVA test followed by Kruskal–Wallis one-way analysis of variance on Ranks with Tukey range test. Probability values of less than 0.05 ($P < 0.05$) were considered significant.

Results and discussion

In recent years, the STAT3 have come to demand the attention of more investigators due to its activation during chronic inflammatory diseases and cancer. Current studies deliver new perception into the biological and molecular mechanisms for the anti-tumor activity of EGCG and myricetin. Previously, it was reported that, inhibitors targeting the SH2 domain of STAT3 obstruct the transcriptional activity of STAT3. The disruption of the translocation dimerization and protein–DNA interactions has the potential to inhibit STAT3 dependent gene expression and thus block its tumor-promoting functions in cancer cells. Nonetheless, there has been less prominence on targeting the STAT3 interface for drug design (Turkson *et al*., 2004, 2005).

Molecular docking of compounds with SH2 domain of STAT3

Recently, molecular docking study of SH2 domain of STAT3 against selected natural compounds has been

Table 2 Evaluation of drug-like properties of the lead molecules by Qikprop Maestro 9.6 molecular docking suite

	Molecule	Q P log $P_{o/w}$ (−2.0 to 6.5)	Q P log HERG (acceptable range: above −5.0)	QPP Caco (nm/s) <25—poor >500—great	Q P log BB (−3 to 1.2)	QPP MDCK (nm/s)	Q Plog Kp (−8.0 to −0.1)
	CID4477	3.081	−5.135	199.07	−1.038	439.272	−3.642
Control	CID114778	3.547	−3.285	2,429.439	−0.105	1,291.327	−1.859
	CID160254	2.775	−3.942	1,724.586	−0.135	891.617	−2.722
	CID252682	0.982	−2.096	7.501	−2.023	3.192	−5.135
	CID2779853	−0.192	−3.939	165.876	−1.007	72.222	−4.193
Anticancer agents	CID252682	1.387	−3.76	6.538	−2.581	2.739	−5.077
	CID5281670	0.371	−4.598	29.617	−2.048	11.022	−5.157
	CID5281672	−0.279	−4.901	7.234	−2.857	2.402	−6.355
	CID72277	−0.193	−4.584	20.527	−2.343	7.416	−5.566
	CID65064	−0.335	−5.474	1.12	−4.172	0.32	−7.477
	STOCK1N-43090	−0.192	−0.789	0.905	−3.134	1.086	−6.023
	STOCK1N-66505	−0.273	−0.245	2.052	−2.198	2.78	−5.547
IBS	STOCK1N-54303	1.478	−0.732	3.423	−2.483	4.338	−5.105
	STOCK1N-44634	−0.337	−0.609	0.593	−3.467	0.602	−6.542
	STOCK1N-45027	0.181	−0.562	3.206	−2.423	4.196	−5.119
	STOCK1N-73784	1.507	−0.928	4.278	−2.269	11.633	−4.371
	STOCK1N-69597	0.519	−3.39	2.319	−1.84	7.464	−5.486
	STOCK1N-73062	−0.043	−4.191	44.06	−1.965	29.978	−4.124
	STOCK1N-81915	1.457	−5.429	224.769	−1.382	98.549	−3.287
	STOCK1N-70844	3.162	−6.229	238.588	−1.505	105.115	−2.813

Predicted IC_{50} value for blockage of HERG K + channels; (acceptable range above −5.0)

Molecule CID, Pubchem IDs; Molecule STOCK, InterBioScreen's library (IBS), Q P log Poct; was predicted partition coefficient of octanol/gas, (8.0 to 35.0); QPP Caco, predicted apparent Caco-2 cell permeability in nm/s. Caco-2 cells is a model for the gut blood barrier (nm/s) <25—poor, >500—great. Q P log BB, predicted brain/blood partition coefficient; QPP MDCK, predicted apparent MDCK cell permeability in nm/s. MDCK cells are considered to be a good mimic for the blood–brain barrier; (nm/s) < 25—poor, >500—great; Q P log KP, Predicted skin permeability; Q P log K_{hsa} Prediction of binding to human serum albumin; (acceptable range −1.5 to 1.5)

carried out. All natural compounds were docked with the X-ray crystal structure of STAT3 (PDB; 1BG1) retrieved from the protein data bank by using Maestro 9.6. Molecular docking stratagem identifies the optimal energy value, types of protein–ligand interactions, possible orientations and conformations of the protein paired with the ligand. The crystal structure of the STAT3 has been determined with 2.25 Å resolutions. Molecular docking result of SH2 domain of STAT3 against natural compounds unveiled that compounds CID252682, CID5281670 (Morin), CID5281672 (Myricetin), CID72277 (Epigallocatechol) and CID65064 (Epigallocatechin Gallate, EGCG) yielded the best Gscore −5.45, −5.03, −4.83, −4.82 and −4.78 kcal/mol, respectively. Moreover, IBS natural compounds STOCK1N-43090, STOCK1N-66505, STOCK1N-54303, STOCK1N-44634, STOCK1N-45027, STOCK1N-73784, STOCK1N-69597, STOCK1N-73062, STOCK1N-81915 and STOCK1N-70844 have better Gscore −6.46, −6.35, −6.29, −6.1, −6.05, −5.87, −5.63, −5.44, −5.18, and −5.1 kcal/mol, respectively. Notable aspects of these compounds are their many pharmacokinetics and pharmacodynamics characteristics are accordance with the lipinski rule of five. Further, in vitro works are carried out to validation of our molecular docking work. The molecular docking study done an aspire to illustrate the protein–ligands interactions and to summarize the various bonds such as hydrogen and electrostatic bond. Protein–ligands interactions profile revealed that SH2 domain of STAT3 amino acid Tyr585, Met586, Leu673, TYR674, Pro675, Ile677 and Ala682 involve in the hydrophobic interactions. Furthermore, amino acid Ser521 and Glu582, involved in side chain hydrogen bond and amino acid Gly583 and Tyr584 included in back-bone hydrogen bond. Moreover, amino acid 518 and Tyr584 form pi-cation and pi–pi-cation interactions, respectively. (Figures 1, 2, 3; Table 1). Molecular docking results divulge that the hydrophobic interactions are the main force for binding of compounds with the SH2 domain of STAT3. Moreover, computer modeling of EGCG bound to the SH2 domain of STAT3 support that the anticancer

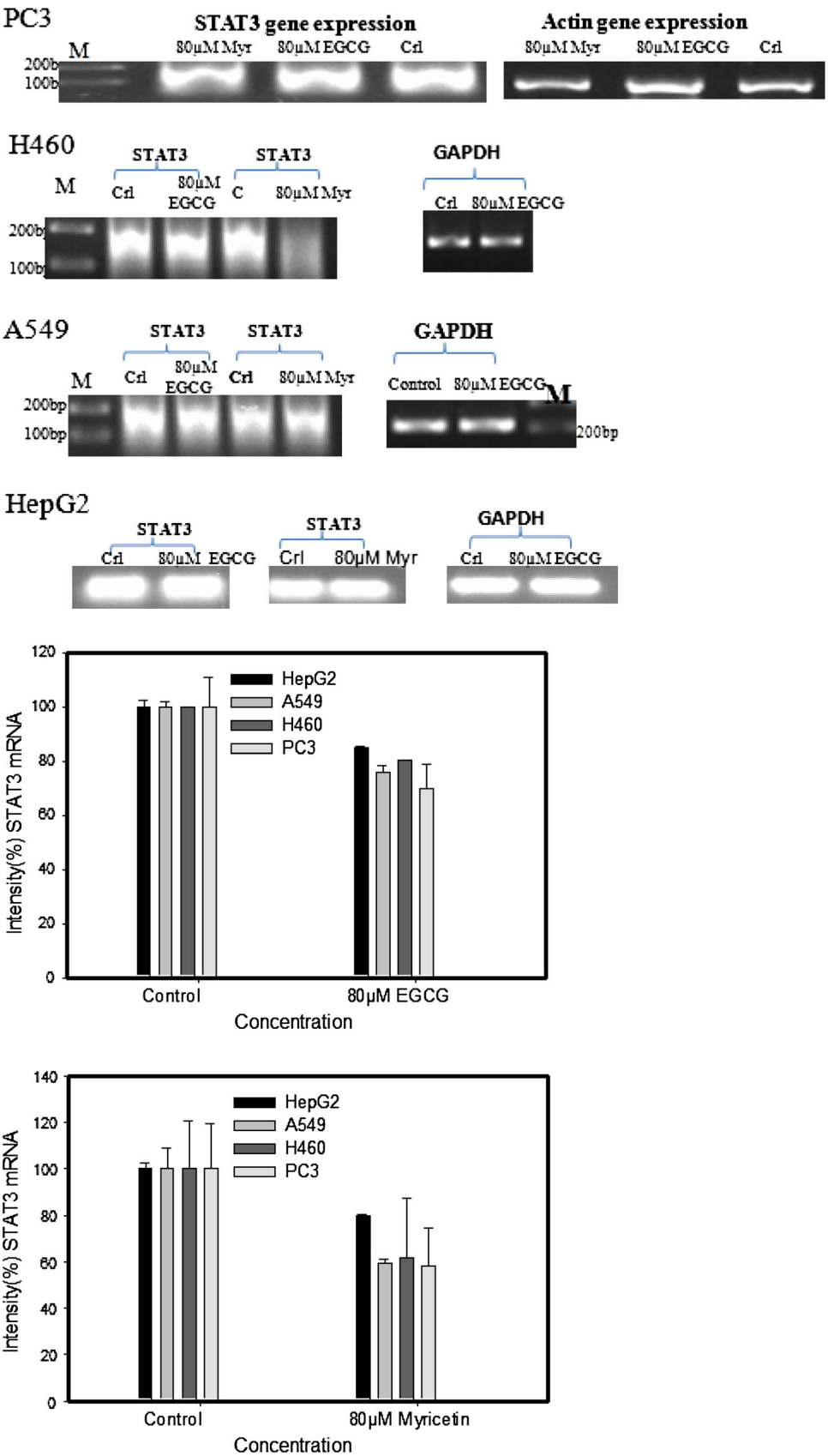

Fig. 4 HepG2, A549, H460 and PC3 cells showed a marked decrease in mRNA expression of STAT3 after the treatment of 80 μM EGCG and myricetin (Myr) alone. Control (Crl)

Table 3 Primer sequences used in study

S. No.	Name of gene	Forward primer (5′ to 3′)	Reverse primer (5′ to 3′)
1	STAT3	ACCCAACAGCCGCCGTAG	CAGACTGGTTGTTTCCATTCAGAT
2	β-Actin	GTGGGGCGCCCCAGGCACCA	CTCCTTAAGTCACGCACGATTTC
3	GAPDH	ACGGATTTGGTCGTATTGGGCG	CTCCTGGAAGATGGTGATGG

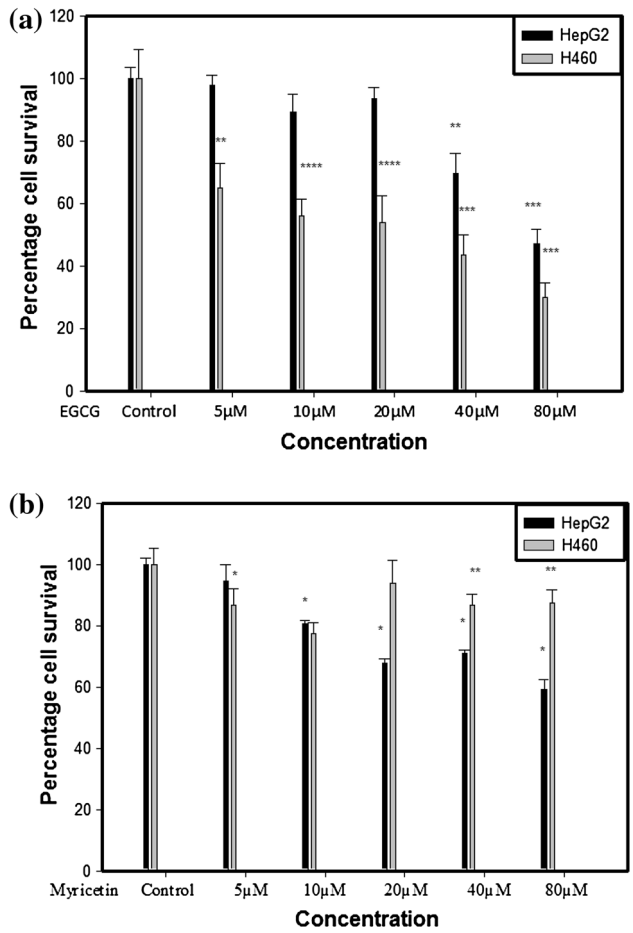

Fig. 5 EGCG and myricetin reduce the cell viability and growth of the HepG2, and H460 cells in a dose-dependent manner determined by the MTT assay (**a**, **b**). $*P < 0.05$ and $**P < 0.01$ versus control

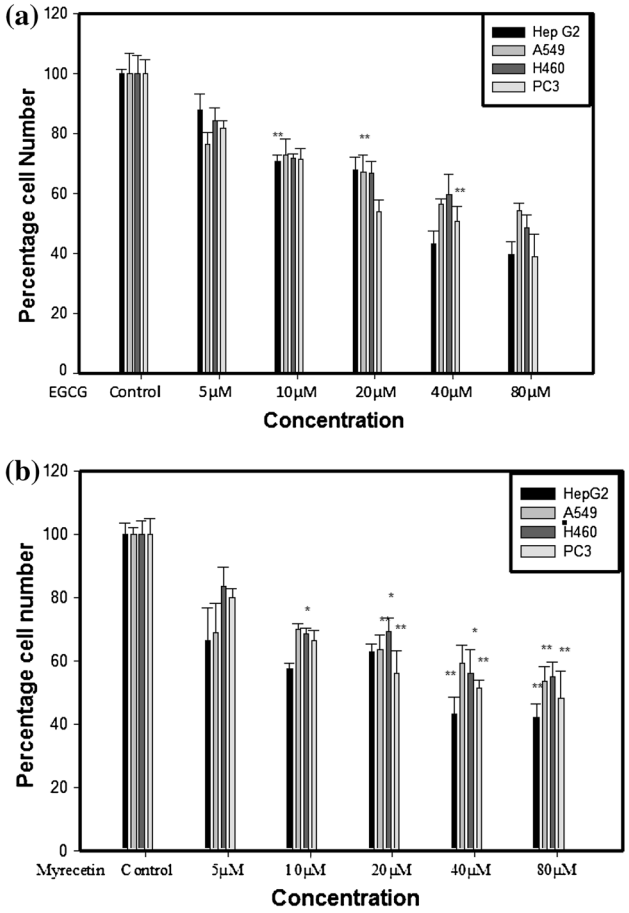

Fig. 6 EGCG and myricetin significantly reduce the cell number on the HepG2, A549, H460, and PC3 cells in a dose-dependent manner determined by the trypan blue exclusion test of cell viability (**a**, **b**). $*P < 0.05$, and $**P < 0.01$ versus control

activity of green tea is the result of the inhibition of the STAT3 signaling pathway (Wang *et al.*, 2013). Seven members of the STAT proteins have been recognized in humans: STAT1, 2, 3, 4, 5a, 5b and 6. All of the STAT proteins share six distinct structural domains, including the N-terminal, coiled-coil, DNA-binding, Src homology 2 (SH2) and the transactivation domains. Present study, we report a natural compound that binds to STAT3 and selectively inactivates STAT3 translocation, dimerization and STAT3 DNA binding (transcription factor activity) that ultimately leads to suppresses of STAT3 dependent malignant transformation.

ADME properties

Pharmacokinetic and pharmacodynamic properties of lead natural compounds were appraised by using the Qikprop application of Maestro 9.6. Compounds CID252682, Morin, Myricetin, Epigallocatechol and EGCG yielded the best Gscore. Most fascinating aspect of these compounds are their admirable QPlogPo/w, QPlogHERGK + channels, QPlogBB, QPlogKP and QPlogKhsa values which satisfy the Lipinski's Rule of Five (Table 2). Moreover, activities such as QPPCaco, QPPMDCK and percentage oral absorption are not satisfactory and structural

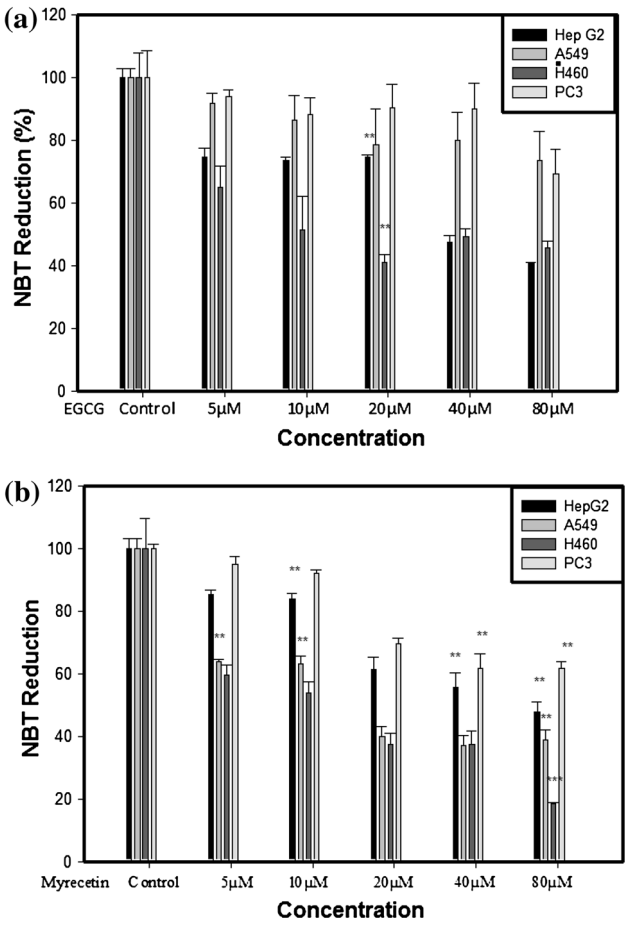

Fig. 7 EGCG and myricetin reduce the ROS on the HepG2, A549, H460, and PC3 cells in a dose-dependent manner determined by the NBT reduction assay (**a**, **b**). $^{*}P < 0.05$, and $^{**}P < 0.01$ versus control

modification is required to enhance these activity. Polar surface area, high oral bioavailability, H-bond donors, and acceptors are imperative criteria for the development for therapeutic agents. It is reported that compounds having 10 or fewer rotatable bonds, and polar surface area equal to or less than 140 Å will have a high probability of good oral bioavailability in the rat. Furthermore, it is also reported that polar surface area inverse proposal to permeation rate (Becker *et al*., 1998). Our best leads molecules EGCG and myricetin have good SASA than control compounds. These results indicate that these compounds will have better permeation rate (Table 2).

A number of reports confirm that EGCG is an efficient anticancer agent that induce apoptosis and decrease cell proliferation via inhibiting STAT3 expression including mesenchymal stromal cells, head and neck squamous cell carcinoma cells and gastric cancer (Lin *et al*., 2012; Zgheib *et al*., 2013; Zhu *et al*., 2011). Moreover, it is reported that myricetin can directly bind to JAK1/STAT3 molecules and modulate the biological signaling that led to inhibit cell transformation in EGF-activated mouse JB6P^{+} cells (Kumamoto *et al*., 2009). Moreover, ex vivo and in vitro pull-down assay unveiled that the myricetin bound to JAK1 and STAT3. However, detailed mechanisms are not disclosed in prostate and lung cancer.

Effect of EGCG and myricetin on STAT3 mRNA expression in cancer cells

We investigated whether EGCG and myricetin could impede STAT3 expression in HepG2, A549, H460 and PC3cells. Cells were incubated for 48 h with EGCG and myricetin and determine the mRNA expression by using RTPCR. Interestingly, RTPCR shows that EGCG and myricetin have a potential for robust inhibition of STAT3. The RTPCR densitometric bands analysis showed that compound EGCG reduced the mRNA expression of STAT3 by 20 % in A549, H460 and PC3 cells at 80 μM concentration, whereas myricetin reduced the mRNA expression of STAT3 by 50 % in A549, H460, and PC3 at 80 μM concentration (Fig. 4). The primer Sequences used in the study listed in Table 3.

Effects of EGCG and myricetin on cell growth of cancer cells

To measure the cytotoxicity of EGCG and myricetin in cancer cells, MTT assay was performed. Cells were cultured with 5, 10, 20, 40 and 80 μM EGCG and myricetin for 48 h. EGCG and myricetin exhibited a remarkable reduction in cell proliferation against cancer cells in a concentration-dependent manner. Consistently, it was more pronounced at concentrations between 5 and 80 μM. The mean 50 % inhibitory concentration of EGCG on cell growth was at 80 μM in HepG2 cells and 20 μM in H460 cells for 48 hrs treatment. It was also observed that cell growth inhibition to 80 μM EGCG in H460 for 48 hrs was 70 %. Furthermore, the mean 40 % inhibitory concentration of myricetin on cell growth was at 80 μM on HepG2 cells for 48 hrs treatment (Fig. 5). Moreover, trypan blue exclusion test of cell viability was performed to determine cell number after the treatments of EGCG and myricetin. EGCG and myricetin revealed a significant reduction of cell number in a concentration-dependent manner (Fig. 6).

The effects of EGCG and myricetin on nitroblue tetrazolium (NBT) reduction on cancer cells

We assessed the ability of the EGCG and myricetin to initiate the production of ROS in cancer cells by using colorimetric nitroblue–tetrazolium (NBT) assay. NBT test is based on the selective reduction in a yellow,

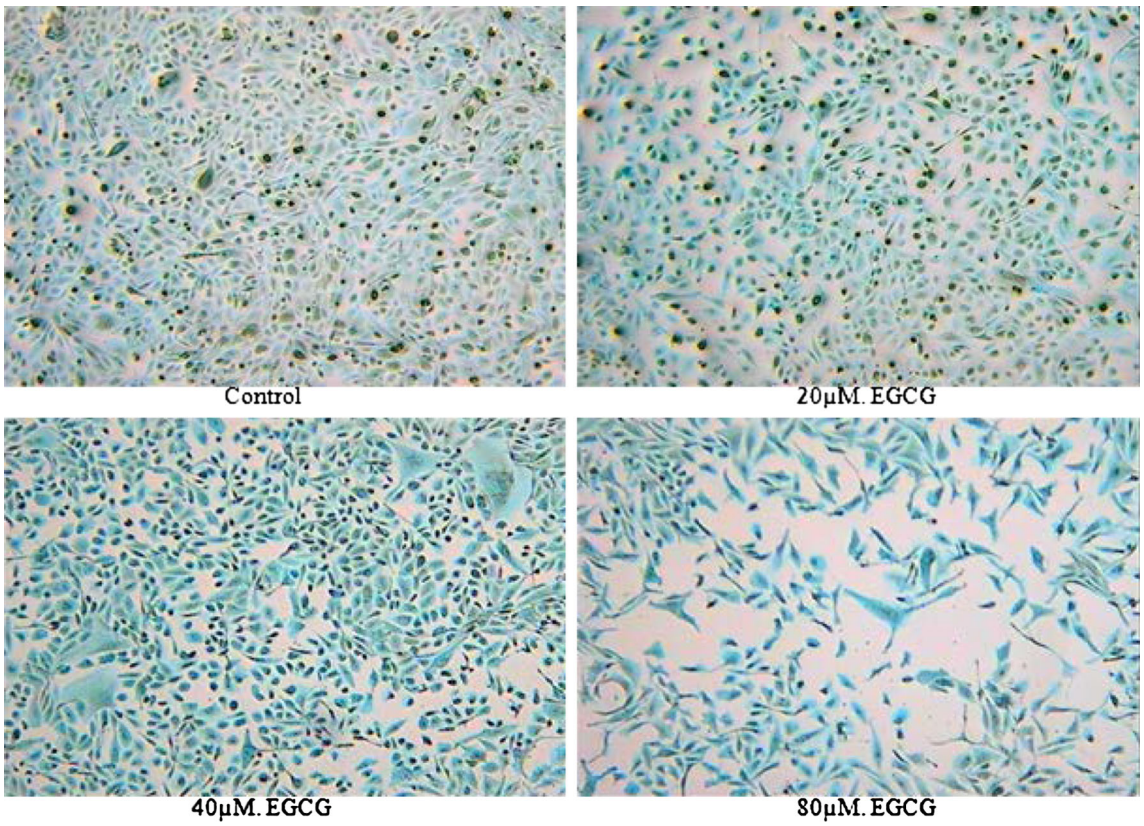

Fig. 8 EGCG inhibits colony formation of PC3 cells. PC3 was grown in six-well plates (1,000 cells/well) in triplicates. After 24 h, incubation removes the media and add FBS-free media (serum starvation). The next day, the media were replaced the culture medium containing 10 % FBS and 20, 40, and 80 μM EGCG. Culture medium was changed once every 3 days for 3 weeks. The pictures of six-well plates with colonies were taken by a Magnus inverted microscope connected to Sony color video camera on day 21

water-soluble tetrazolium chloride to an insoluble violet diformazan by superoxide. In cancer cells, the EGCG and myricetin caused a reduction in ROS generation that led to reduced cell proliferation. We noticed a lung cancer cells are most sensitive for ROS production and reduction in ROS on both lung cancer cells approximately 60 % on above 20 μM concentration. Treatment of EGCG and myricetin on cancer cell led to the significant reduction in ROS (Fig. 7).

EGCG and myricetin reduce colony formation of prostate cancer cell (PC3) in vitro

We next studied the ability of PC3 cells to form colonies on 6-well culture plates in the presence or absence of EGCG and myricetin for 3 weeks. EGCG and myricetin reduced colony formation at concentrations as 20–80 μM. The number of colonies formed was reduced in a dose-dependent manner. At the highest concentration of EGCG and myricetin (80 μM), colony formation was reduced over 50 % as compared to the untreated controls (Figs. 8, 9). EGCG has been reported to impede lipid peroxidation and expression of colony-stimulating factors compromised in several pathologic conditions by using membrane matrix metalloproteinase (Zgheib *et al*., 2013).

A number of in vitro, in vivo and clinical studies have reveal that EGCG can induce apoptosis, and inhibit invasion and metastasis of prostate, lung and hepatic cancer cells (Connors *et al*., 2012; Mereles and Hunstein, 2011; Shim *et al*., 2010). Furthermore, proteasome inhibition treating prostate cancer cell lines with EGCG led to the accumulation of the cyclin-dependent kinase inhibitor, which ultimately result in cell cycle arrest (Nam *et al*., 2001). The study demonstrated that the combination of myricetin with radiotherapy can enhance tumor radiosensitivity of A549 and H1299 cells (Zhang *et al*., 2014). Furthermore, treatment of EGCG modulate the activity of phosphatidylinositol-3-kinase (PI3K) and mitogen-activated protein kinase (MAPK) pathways and found to decrease the levels of PI3K and phospho-Akt in hepatocellular, prostate cancer cells (Shen *et al*., 2014; Siddiqui *et al*., 2004). Myricetin acts as PI3KϒΥ inhibitor with

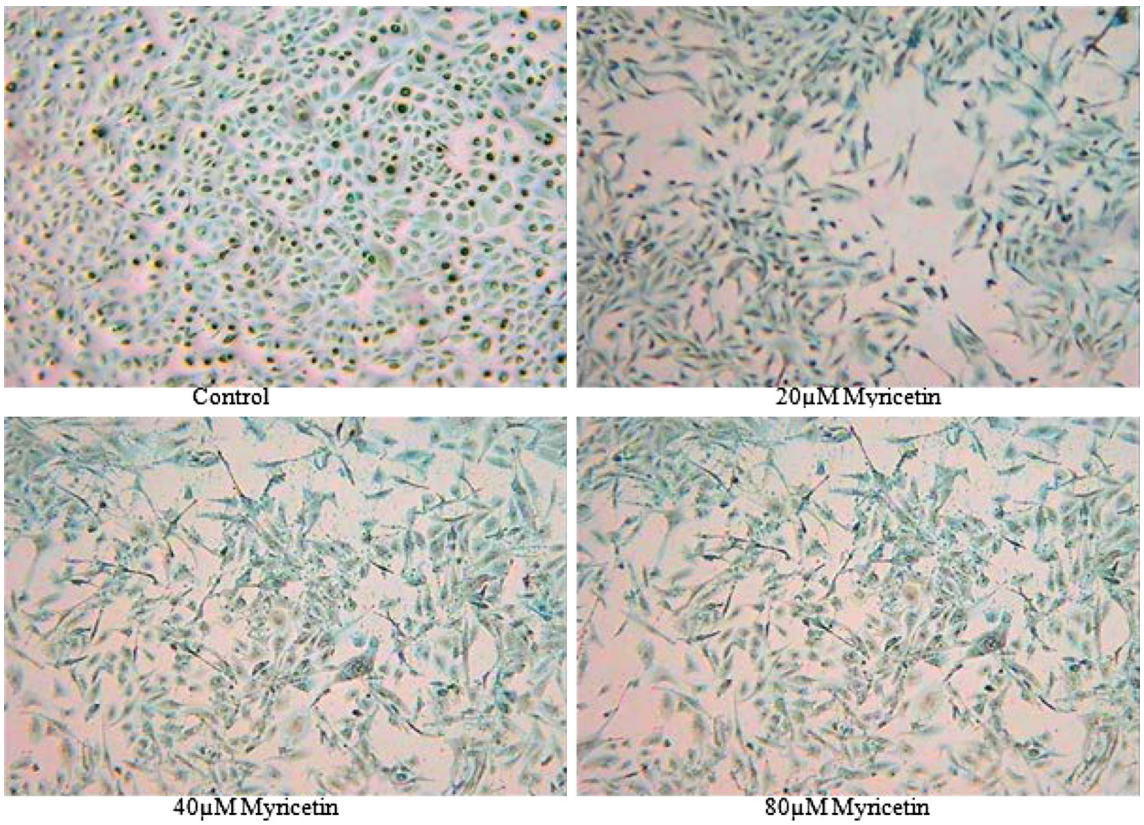

Fig. 9 Myricetin inhibits colony formation of PC3 cells. PC3 was grown in six-well plates (1,000 cells/well) in triplicates. After 24 h, incubation media were removed, and FBS-free media added (serum starvation). The next day, the media were replaced the culture medium containing 10 % FBS and 20, 40 and 80 μM myricetin. Culture medium was changed once every 3 days for 3 weeks. The pictures of six-well plates with colonies were taken by a Magnus inverted microscope connected to Sony color video camera on day 21

dissociation constants (Kd) of 0.17 μM (Walker *et al*., 2000). Furthermore, it is reported that myricetin stimulate pancreatic cancer cell death in vitro via reducing PI3K activity (Phillips *et al*., 2011). Our previous article shows that compounds myricetin have the best Gscore when docked with Akt, PDK1 and PI3K, whereas EGCG have better Gscore when docked with PI3K and mTOR (Singh and Bast, 2014b). Molecular docking between EGCG with STAT3 SH2 shown that amino acid Lys591, Lys591, Glu594, Arg609, Ser611, Glu612, Ser613,-Ser613, Thr620, Val637, Glu638 and Pro639 involved in protein–ligands interactions of EGCG with SH2 domain of STAT3 (Wang *et al*., 2013). Previous report disclosed that myricetin inhibited DNA-binding and transcriptional activity of STAT3 via inhibited the phosphorylation of STAT3 at Tyr705 and Ser727 (Kumamoto *et al*., 2009). Schematic model representations for the inhibition of STAT3 signaling by EGCG and myricetin shown on Fig. 10. EGCG and myricetin bind to SH2 domain of STAT3 that block the STAT3 translocation, dimerization and STAT3-DNA binding (transcription factor activity) that ultimately leads to suppresses of STAT3-dependent malignant transformation.

Moreover, members of the STAT family range in size from 750 to 900 amino acids and contain several structural domains including SH2 domain coiled-coil, DNA-binding, linker, tyrosine activation and transcriptional activation domains. In this context, further molecular docking study of DNA-binding domain of STAT3 against selected natural compounds has been carried out. Molecular docking result of DNA-binding domain of STAT3 against natural compounds unveiled that EGCG and myricetin, STOCK1N-50253 and STOCK1N-03390 compounds have better Gscore −10.12, −9.54, −13.15 and −10.05 kcal/mol, respectively. Protein–ligands interactions profile revealed that DNA-binding domain of STAT3 amino acid Asp374, Val375, Leu378, Arg379, Ser381, Arg382, Gln416, Cys418, Asn420, Leu430, Arg423 and Glu435 involves in the hydrogen bond and π–π stacking interactions in addition to hydrophobic interactions (supplementary table 2). Further, in vitro and in vivo works are required for validation of our molecular docking work.

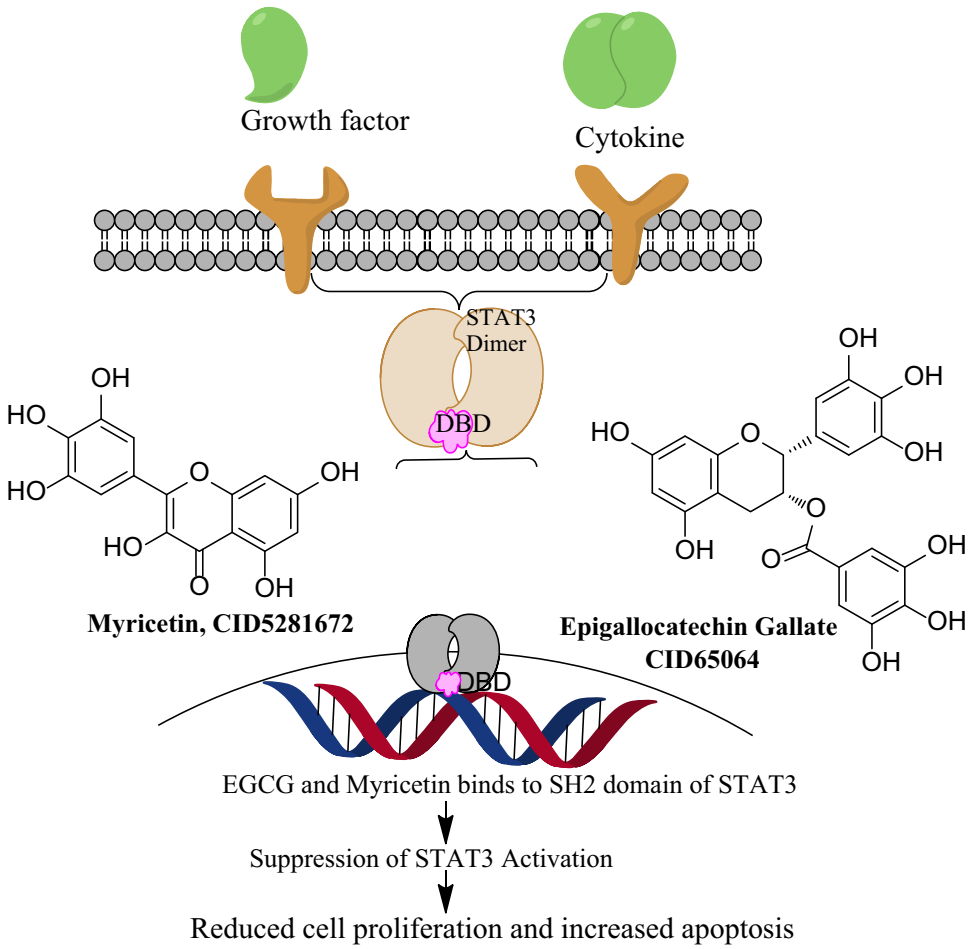

Fig. 10 Schematic model presentations for the inhibition of STAT3 signaling by EGCG and myricetin. EGCG and myricetin bind to SH2 domain of STAT3 that block the STAT3 translocation, dimerization and STAT3-DNA binding (transcription factor activity) that ultimately leads to suppresses of STAT3 dependent malignant transformation

Conclusion

STAT3 pathway is a master regulator of many extracellular cytokine signals, insulin, and IGF, which are involved in maintaining growth and development. Constitutively activated STAT3 are involved in aberrant signaling pathways which turn normal cellular processes to transformed state. In this study, we aimed to identify STAT3 inhibitors by using Maestro 9.6 molecular docking suite. Molecular docking result of SH2 domain of STAT3 against natural compounds disclose that compounds CID252682, Morin, Myricetin, Epigallocatechol, and EGCG yielded the best Gscore −5.45, −5.03, −4.83, −4.82, and −4.78 kcal/mol, respectively as well as binding conformation. Moreover, IBS natural compounds STOCK1N-43090, STOCK1N-66505, STOCK1N-54303, STOCK1N-44634, STOCK1N-45027, STOCK1N-73784, STOCK1N-69597, STOCK1N-73062, STOCK1N-81915 and STOCK1N-70844 had better binding energy −6.46, −6.35, −6.29, −6.1, −6.05, −5.87, −5.63, −5.44, −5.18, and −5.1 kcal/mol, respectively. Protein–ligand interactions are disclosed that SH2 domain of STAT3 amino acid Tyr585, Met586, Leu673, TYR674, Pro675, Ile677 and Ala682 involve in the hydrophobic interactions. Furthermore, amino acid Ser521 and Glu582 involved in side chain hydrogen bond and amino acid Gly583 and Tyr584 involved in back-bone hydrogen bond. Moreover, amino acid 518 and Tyr584 form pi-cation and pi–pi-cation interactions, respectively. Foremost, these compounds had excellent QPlogPo/w, QPlogHERGK + channels, QPlogBB, QPlogKP and QPlogKhsa values which satisfy the lipinski's rule of five. Moreover, activities such as QPPCaco, QPPMDCK and percentage oral absorption are not satisfactory, structural modification is required to enhance the activity. EGCG and myricetin reduce the STAT3 mRNA expression, as confirmed by RTPCR. Moreover, EGCG and myricetin reduce cell proliferation and ROS generation after the 48 h treatments of EGCG and myricetin alone. Interestingly, our result also indicates that reduction in potential of colony formation enhances anti-metastasis activity of EGCG and myricetin. However, further in vivo and in vitro studies are required for understanding detailed molecular mechanisms.

Acknowledgments We would like to thank Vice Chancellor, Central University of Punjab, Bathinda, Punjab, (India) for supporting this study with infrastructural requirements. We also thank Professor P. Ramarao (Dean, Academic Affairs), Central University of Punjab, Bathinda, Punjab, India, for his suggestions during the course that tremendously helped to improve this article. This study was also supported by a Senior Research Fellowship Grant-in-Aid from Indian Council of Medical Research (ICMR), Government of India awarded to PS.

Conflict of interest The authors declare that there is no conflict of interests regarding the publication of this article.

References

Aggarwal BB, Kunnumakkara AB, Harikumar KB, Gupta SR, Tharakan ST, Koca C, Dey S, Sung B (2009) Signal transducer and activator of transcription-3, inflammation, and cancer. Ann N Y Acad Sci 1171:59–76

Alimova IN, Liu B, Fan Z, Edgerton SM, Dillon T, Lind SE, Thor AD (2009) Metformin inhibits breast cancer cell growth, colony formation and induces cell cycle arrest in vitro. Cell Cycle 8:909–915

Azare J, Leslie K, Al-Ahmadie H, Gerald W, Weinreb PH, Violette SM, Bromberg J (2007) Constitutively activated Stat3 induces tumorigenesis and enhances cell motility of prostate epithelial cells through integrin β6. Mol Cell Biol 27:4444–4453

Becker S, Groner B, Müller CW (1998) Three-dimensional structure of the Stat3β homodimer bound to DNA. Nature 394:145–151

Bhanot A, Sharma R, Noolvi MN (2011) Natural sources as potential anti-cancer agents: a review. Int J Phytomed 3:09–26

Bill A, Schmitz A, König K, Heukamp LC, Hannam JS, Famulok M (2012) Anti-proliferative effect of cytohesin inhibition in Gefitinib-resistant lung cancer cells. PLoS ONE 7:e41179

Cho JY, Park J (2008) Contribution of natural inhibitors to the understanding of the PI3K/PDK1/PKB pathway in the insulin-mediated intracellular signaling cascade. Int J Mol Sci 9:2217–2230

Chung CD, Liao J, Liu B, Rao X, Jay P, Berta P, Shuai K (1997) Specific inhibition of Stat3 signal transduction by PIAS3. Science 278:1803–1805

Connors SK, Chornokur G, Kumar NB (2012) New insights into the mechanisms of green tea catechins in the chemoprevention of prostate cancer. Nutr Cancer 64:4–22

Cragg GM, Newman DJ (2005) Plants as a source of anti-cancer agents. J Ethnopharmacol 100:72–79

Da Rocha AB, Lopes RM, Schwartsmann G (2001) Natural products in anticancer therapy. Curr Opin Pharmacol 1:364–369

Dave B, Landis MD, Dobrolecki LE, Wu M-F, Zhang X, Westbrook TF, Hilsenbeck SG, Liu D, Lewis MT, Tweardy DJ (2012) Selective small molecule stat3 inhibitor reduces breast cancer tumor-initiating cells and improves recurrence free survival in a human-xenograft model. PLoS ONE 7:e30207

Debnath B, Xu S, Neamati N (2012) Small molecule inhibitors of signal transducer and activator of transcription 3 (Stat3) protein. J Med Chem 55:6645–6668

Fletcher S, Turkson J, Gunning PT (2008) Molecular approaches towards the inhibition of the signal transducer and activator of transcription 3 (Stat3) protein. ChemMedChem 3:1159–1168

Friedbichler K, Kerenyi MA, Müllner EW, Moriggl R (2009) Stat5 as hematopoietic gatekeeper and oncogene upon tyrosine kinase-induced transformation. JAK-STAT Pathw Dis 131

Friesner RA, Banks JL, Murphy RB, Halgren TA, Klicic JJ, Mainz DT, Repasky MP, Knoll EH, Shelley M, Perry JK (2004) Glide: a new approach for rapid, accurate docking and scoring. 1. Method and assessment of docking accuracy. J Med Chem 47:1739–1749

Friesner RA, Murphy RB, Repasky MP, Frye LL, Greenwood JR, Halgren TA, Sanschagrin PC, Mainz DT (2006) Extra precision glide: docking and scoring incorporating a model of hydrophobic enclosure for protein–ligand complexes. J Med Chem 49:6177–6196

Gooch JL, Christy B, Yee D (2002) STAT6 mediates interleukin-4 growth inhibition in human breast cancer cells. Neoplasia 4:324

Grivennikov SI, Karin M (2010) Dangerous liaisons: STAT3 and NF-κB collaboration and crosstalk in cancer. Cytokine Growth Factor Rev 21:11–19

Halgren TA, Murphy RB, Friesner RA, Beard HS, Frye LL, Friesner RA, Murphy RB, Repasky MP, Frye LL, Greenwood JR, Halgren TA, Sanschagrin PC, Mainz DT et al (2004) Glide: a new approach for rapid, accurate docking and scoring. 2. Enrichment factors in database screening. J Med Chem 47: 1750–1759

Hillman GG (2012) Dietary agents in cancer chemoprevention and treatment. J Ooncology

Huang AJ, Moffat B, Yansura DG (2005a) Heteromultimeric molecules. Google Patents

Huang HF, Murphy TF, Shu P, Barton AB, Barton BE (2005b) Stable expression of constitutively-activated STAT3 in benign prostatic epithelial cells changes their phenotype to those resembling malignant cells. Mol Cancer 4

Huang W, He T, Chai C, Yang Y, Zheng Y, Zhou P, Qiao X, Zhang B, Liu Z, Wang J (2012) Triptolide inhibits the proliferation of prostate cancer cells and down-regulates SUMO-specific protease 1 expression. PLoS ONE 7:e37693

Jorgensen WL, Duffy EM (2002) Prediction of drug solubility from structure. Adv Drug Deliv Rev 54:355–366

Jorgensen WL, Tirado-Rives J (1988) The OPLS [optimized potentials for liquid simulations] potential functions for proteins, energy minimizations for crystals of cyclic peptides and crambin. J Am Chem Soc 110:1657–1666

Jorgensen WL, Maxwell DS, Tirado-Rives J (1996) Development and testing of the OPLS all-atom force field on conformational energetics and properties of organic liquids. J Am Chem Soc 118:11225–11236

Kumamoto T, Fujii M, Hou D-X (2009) Myricetin directly targets JAK1 to inhibit cell transformation. Cancer Lett 275:17–26

Lin H-Y, Hou S-C, Chen S-C, Kao M-C, Yu C-C, Funayama S, Ho C-T, Way T-D (2012) (−)-Epigallocatechin gallate induces Fas/CD95-mediated apoptosis through inhibiting constitutive and IL-6-induced JAK/STAT3 signaling in head and neck squamous cell carcinoma cells. J Agric Food Chem 60:2480–2489

Liu B, Ordonez-Ercan D, Fan Z, Edgerton SM, Yang X, Thor AD (2007) Downregulation of erbB3 abrogates erbB2-mediated tamoxifen resistance in breast cancer cells. Int Cancer 120:1874–1882

Lu JJ, Crimin K, Goodwin JT, Crivori P, Orrenius C, Xing L, Tandler PJ, Vidmar TJ, Amore BM, Wilson AG (2004) Influence of molecular flexibility and polar surface area metrics on oral bioavailability in the rat. J Med Chem 47:6104–6107

Mereles D, Hunstein W (2011) Epigallocatechin-3-gallate (EGCG) for clinical trials: more pitfalls than promises? Int J Mol Sci 12:5592–5603

Nam S, Smith DM, Dou QP (2001) Ester bond-containing tea polyphenols potently inhibit proteasome activity in vitro and in vivo. J Biol Chem 276:13322–13330

Ni Z, Lou W, Leman ES, Gao AC (2000) Inhibition of constitutively activated Stat3 signaling pathway suppresses growth of prostate cancer cells. Cancer Res 60:1225–1228

Niu G, Heller R, Catlett-Falcone R, Coppola D, Jaroszeski M, Dalton W, Jove R, Yu H (1999) Gene therapy with dominant-negative Stat3 suppresses growth of the murine melanoma B16 tumor in vivo. Cancer Res 59:5059–5063

Niu G, Shain KH, Huang M, Ravi R, Bedi A, Dalton WS, Jove R, Yu H (2001) Overexpression of a dominant-negative signal transducer and activator of transcription 3 variant in tumor cells leads to production of soluble factors that induce apoptosis and cell cycle arrest. Cancer Res 61:3276–3280

Phillips P, Sangwan V, Borja-Cacho D, Dudeja V, Vickers S, Saluja A (2011) Myricetin induces pancreatic cancer cell death via the induction of apoptosis and inhibition of the phosphatidylinositol 3-kinase (PI3K) signaling pathway. Cancer Lett 308: 181–188

Phosrithong N, Ungwitayatorn J (2010) Molecular docking study on anticancer activity of plant-derived natural products. Med Chem Res 19:817–835

Rawlings JS, Rosler KM, Harrison DA (2004) The JAK/STAT signaling pathway. J Cell Sci 117:1281–1283

Roell D, Baniahmad A (2011) The natural compounds atraric acid and N-butylbenzene-sulfonamide as antagonists of the human androgen receptor and inhibitors of prostate cancer cell growth. Mol Cell Endocrinol 332:1–8

Sarkar FH, Li Y (2006) Using chemopreventive agents to enhance the efficacy of cancer therapy. Cancer Res 66:3347–3350

Schindler C, Levy DE, Decker T (2007) JAK-STAT signaling: from interferons to cytokines. J Biol Chem 282:20059–20063

Shen X, Zhang Y, Feng Y, Zhang L, Li J, Xie Y-A, Luo X (2014) Epigallocatechin-3-gallate inhibits cell growth, induces apoptosis and causes S phase arrest in hepatocellular carcinoma by suppressing the AKT pathway. Int J Oncol 44:791–796

Shim J-H, Su Z-Y, Chae J-I, Kim DJ, Zhu F, Ma W-Y, Bode AM, Yang CS, Dong Z (2010) Epigallocatechin gallate suppresses lung cancer cell growth through Ras–GTPase-activating protein SH3 domain-binding protein 1. Cancer Prev Res 3:670–679

Shivakumar D, Williams J, Wu Y, Damm W, Shelley J, Sherman W (2010) Prediction of absolute solvation free energies using molecular dynamics free energy perturbation and the OPLS force field. J Chem Theory Comput 6:1509–1519

Siddiqui IA, Adhami VM, Afaq F, Ahmad N, Mukhtar H (2004) Modulation of phosphatidylinositol-3-kinase/protein kinase B, and mitogen-activated protein kinase-pathways by tea polyphenols in human prostate cancer cells. J Cell Biochem 91:232–242

Simon AR, Rai U, Fanburg BL, Cochran BH (1998) Activation of the JAK-STAT pathway by reactive oxygen species. Am J Physiol Cell Physiol 275:C1640–C1652

Singh P, Bast F (2014a) *In silico* molecular docking study of natural compounds on wild and mutated epidermal growth factor receptor. Med Chem Res 23:5074–5085

Singh P, Bast F (2014b) Multitargeted molecular docking study of plant-derived natural products on phosphoinositide-3 kinase pathway components. Med Chem Res 23:1690–1700

Sunil H (2012) Inhibition studies of naturally occurring terpene based compounds with cyclin-dependent kinase 2 enzyme. J Comput Sci Syst Bio 5:2

Takeda K, Akira S (2000) STAT family of transcription factors in cytokine-mediated biological responses. Cytokine Growth Factor Rev 11:199–207

Takeda K, Noguchi K, Shi W, Tanaka T, Matsumoto M, Yoshida N, Kishimoto T, Akira S (1997) Targeted disruption of the mouse Stat3 gene leads to early embryonic lethality. Proc Natl Acad Sci USA 94:3801

Turkson J, Zhang S, Palmer J, Kay H, Stanko J, Mora LB, Sebti S, Yu H, Jove R (2004) Inhibition of constitutive signal transducer and activator of transcription 3 activation by novel platinum complexes with potent antitumor activity. Mol Cancer Ther 3:1533–1542

Turkson J, Zhang S, Mora LB, Burns A, Sebti S, Jove R (2005) A novel platinum compound inhibits constitutive Stat3 signaling and induces cell cycle arrest and apoptosis of malignant cells. J Biol Chem 280:32979–32988

Walker EH, Pacold ME, Perisic O, Stephens L, Hawkins PT, Wymann MP, Williams RL (2000) Structural determinants of phosphoinositide 3-kinase inhibition by wortmannin, LY294002, quercetin, myricetin, and staurosporine. Mol Cell 6(4):909–919

Wang Y, Ren X, Deng C, Yang L, Yan E, Guo T, Li Y, Xu MX (2013) Mechanism of the inhibition of the STAT3 signaling pathway by EGCG. Oncol Rep 30:2691–2696

Watowich SS, Hilton DJ, Lodish HF (1994) Activation and inhibition of erythropoietin receptor function: role of receptor dimerization. Mol Cell Bio 14:3535–3549

Yu H, Kortylewski M, Pardoll D (2007) Crosstalk between cancer and immune cells: role of STAT3 in the tumour microenvironment. Nat Rev Immunol 7:41–51

Yu H, Pardoll D, Jove R (2009) STATs in cancer inflammation and immunity: a leading role for STAT3. Nat Rev Cancer 9:798–809

Yue P, Turkson J (2009) Targeting STAT3 in cancer: how successful are we? Expert Opin Investig Drugs

Zgheib A, Lamy S, Annabi B (2013) Epigallocatechin gallate targeting of membrane type 1 matrix metalloproteinase-mediated Src and Janus kinase/signal transducers and activators of transcription 3 signaling inhibits transcription of colony-stimulating factors 2 and 3 in mesenchymal stromal cells. J Biol Chem 288:13378–13386

Zhang M, Zhu W, Ding N, Zhang W, Li Y (2013) Identification and characterization of small molecule inhibitors of signal transducer and activator of transcription 3 (STAT3) signaling pathway by virtual screening. Bioorg Med Chem Lett 23:2225–2229

Zhang S, Wang L, Liu H, Zhao G, Ming L (2014) Enhancement of recombinant myricetin on the radiosensitivity of lung cancer A549 and H1299 cells. Diagn Pathol 9:68

Zhu B-H, Chen H-Y, Zhan W-H, Wang C-Y, Cai S-R, Wang Z, Zhang C-H, He Y-L (2011) (-)-Epigallocatechin-3-gallate inhibits VEGF expression induced by IL-6 via Stat3 in gastric cancer. World J Gastroenterol 17:2315